applied sciences

MDPI

Article

Employing Discrete Solid Phases to Represent C-S-H Solid Solutions in the Cemdata07 Thermodynamic Database to Model Cement Hydration Using the PHREEQC Geochemical Software

Niall Holmes [1,2,*], Mark Tyrer [1,2] and Denis Kelliher [3]

[1] School of Civil & Structural Engineering, Technological University Dublin, D07 EWV4 Dublin, Ireland
[2] Institute of Advanced Study, Collegium Basilea, 4053 Basel, Switzerland
[3] Department of Civil & Environmental Engineering, University College Cork, T12 K8AF Cork, Ireland
* Correspondence: niall.holmes@tudublin.ie; Tel.: +353-(0)-1-220-6678

Abstract: This paper presents a cement hydration model over time using the cemdata07 thermodynamic database and a series of derived discrete solid phases (DSPs) to represent calcium silicate hydrate (C-S-H) as a binary solid solution with two end-members. C-S-H in cement is amorphous and poorly crystalline with a range of molar Ca/Si ratios from 0.6 to 1.7. It displays strongly incongruent dissolution behaviour, where the release of calcium into solution is several orders of magnitude greater than silicon. It is, therefore, important that any cement hydration model provides a credible account of this behaviour. C-S-H has been described in the cemdata07 thermodynamic database as a number of solid solutions using different end-members with differing levels of complexity. While solid solutions can be included in most modern geochemical software programs, they often lead to a significant increase in computation time. This paper presents how an incongruent solid solution between two C-S-H end-members may be represented as a number of DSPs to model cement hydration over time using the PHREEQC geochemical software. By using DSPs rather than modelling C-S-H as a nonideal solid solution, this gives the user full control of the input for the model, reducing the computational demand and analysis time with no loss in accuracy in predicting stable-phase assemblages and their associated pore chemistry over time.

Keywords: cement; hydration; solid solutions; thermodynamics; modelling

Citation: Holmes, N.; Tyrer, M.; Kelliher, D. Employing Discrete Solid Phases to Represent C-S-H Solid Solutions in the Cemdata07 Thermodynamic Database to Model Cement Hydration Using the PHREEQC Geochemical Software. *Appl. Sci.* **2022**, *12*, 10039. https://doi.org/10.3390/app121910039

Academic Editor: Doo-Yeol Yoo

Received: 21 September 2022
Accepted: 2 October 2022
Published: 6 October 2022

1. Introduction

Predictions of solid hydrate formation and pore solution chemistry over time using thermodynamic modelling has been shown to be a reliable method by several authors for many cement systems. To simulate hydration using thermodynamics requires descriptions of the solids and dissolved species in the system, along with data on the clinker oxide proportions, water/cement (w/c) ratio, curing temperature, relative humidity and Blaine fineness of the cement. To accurately model hydration over time, empirical rate equations are used to describe the dissolution of OPC clinker phases. Oxide components dissolved in the OPC clinker phases, the oversaturation of specific phases during the first 12 h of hydration and the release and uptake of alkali elements (K and Na) by C-S-H are also believed to produce accurate predictions.

The widely used and freely available geochemical software PHREEQC has been shown by the authors of [1] to be capable of predicting the hydration behaviour of Portland cement over time using an appropriate thermodynamic database and the molar reaction equations for the four main clinker phases alite (Ca_3SiO_5, C_3S), belite (Ca_2SiO_4, C_2S), aluminate ($Ca_3Al_2O_6$, C_3A) and aluminoferrite ($Ca_4Al_2Fe_3O_{10}$, C_4AF). PHREEQC employs the law of mass action equations to perform complex geochemical simulations, allowing for the inclusion of kinetics and rates, details of which can be found in the literature [2–10].

C-S-H in cement is amorphous and poorly crystalline with a range of molar Ca/Si ratios between 0.6 and 1.7. It displays strongly incongruent dissolution behaviour, where the release of calcium into solution is several orders of magnitude greater than that of silicon. It is, therefore, important that any cement hydration model used to predict stable-phase assemblages, pH and pore chemistries over time employs a suitable C-S-H gel solubility model to accurately describe its variable composition and solubility behaviour. An example of this incongruent dissolution behaviour is given in [11].

Solid solutions are homogeneous crystalline structures where one or more component can be partly or wholly substituted on specific lattice sites with moieties of equivalent charge. If the host and substituting moieties are chemically similar, the formation of an ideal solid solution is possible. However, as is often the case, differences are sufficiently large enough to cause the formation of a nonideal solid solution, which can be readily confirmed by the appearance of a miscibility gap [12]. Solid solutions are of great importance in cement chemistry, where they can be used to describe the strongly incongruent dissolution behaviour of calcium silicate hydrate (C-S-H) gel [13,14], the substitution of SiO_4^{4-} and $4OH^-$ in hydrogarnets [15–17] and the substitution of cationic Al^{3+} and Fe^{3+} and anionic $2OH^-$, $2Cl^-$, SO_4^{2-} and CO_3^{2-} components in AFt and AFm minerals [15–17].

If the thermodynamic properties of the unsubstituted and pure end-members are known, it is possible to calculate a series of DSPs that can be used to provide a credible thermodynamic model of cement hydration. Work by [18] demonstrates that DSPs can be derived for any ideal or nonideal solid solution. For example, [19] developed a DSP C-S-H gel solubility model based on two binary, nonideal, solid solutions that yielded satisfactory predictions of pH, Ca and Si concentrations for molar Ca/Si (C/S) ratios from 0 to 2.7, the occurrence of portlandite at C/S > 1.65, amorphous silica at C/S < 0.55 and congruent dissolution at C/S = 0.85. Previous work employing the density functional theory (DFT) [20,21] developed thermodynamic predictions for silicate hydrates and other chemical systems and provided accurate predictions of thermochemistry using constitutive models.

In the current paper, DSPs are derived for the jennite and tobermorite-II C-S-H gel solubility models in cemdata07 [7] and used to predict ordinary Portland cement (OPC) hydration as a function of time using the geochemical code PHREEQC. The results are compared to the experimentally supported GEM predictions from [22] using cemdata07 to provide comparisons. While a newer version of the cemdata07 database is now available [23], and other solid solution models are available, such as CSH-3T and CSHQ [23], the cemdata07 database and the jennite and tobermorite-II C-S-H gel solubility models are used here to demonstrate the accuracy of the DSP approach and how it can be simply applied in PHREEQC to model cement hydration. It is shown how this methodology gives the user full control of the input for the model with a faster follow-on analysis time and, most importantly, no loss in accuracy in the prediction of phase assemblages and pore chemistry as hydration continues.

2. Derivation of Discrete Solid Phases (DSPs) from Cemdata07 Solid Solution End-Members

The first step in deriving a series of DSPs was defining the pure end-members and their thermodynamic properties in terms of Gibbs free energy (G, J/mol), enthalpy (H, J/mol), entropy (S, J/K/mol), heat capacity (Cp, J/K/mol) and molar volume (V, cm^3/mol) (see Table 1) [7]. These thermodynamic properties could then be used to calculate the solubility constant, log K and its variation with temperature for the dissolution reactions of each end-member (Table 2). As shown, the end-members were listed in order of increasing solubility and the analytical expressions described the variation of log K as a function of temperature (in Kelvin) where a, c and d were calculated using Equation (1) as functions of enthalpy (ΔrH, J/mol), entropy (ΔrS, J/K/mol) and heat capacity (ΔrCp, J/K/mol) of reaction [7], b, e and f = 0, and T denotes temperature. Each of the

end-members shown in Table 2 and their respective analytical expressions were written directly into PHREEQC to suit its data input syntax.

$$\log K = a + b \cdot T + c/T + d \cdot \log10(T) + e \cdot T^{-2} + f \cdot T^{2} \quad (1)$$

Table 1. Thermodynamic properties of tobermorite-II and jennite as taken from the cemdata07 database [7]. Letters assigned to each end-member are shown in parentheses.

Component	G [i]	H [i]	S [ii]	Cp [ii]
Tobermorite-II	−1,744,356	−1,915,813.3	80	132.372
Jennite	−2,480,808	−2,723,484.3	140	210.805
Ca^{+2}	−552,790	−543,069	−56.483997	−30.922515
SiO_2(aq)	−833,411	−887,856.17	41.338001	44.465416
H_2O	−237,183	−285,881	69.923	75.3605
H^+	0	0	0	0

[i] J/mol. [ii] J/mol/K. Molar volumes for tobermorite-II and jennite taken as 59 cm^3/mol and 78 cm^3/mol, respectively.

Table 2. End-members and DSP for the CSH model.

Phase	Mole Fraction		DSP Dissolution Reactions	Log K (25 °C)	Analytical Expression Parameters (Equation (1))			Vol (cm^3/mol)
	X_i	X_j			a	C	d	
Tobermorite II	1	0	(CaO)0.8333(SiO_2)1.0000(H_2O) 1.3330 + 1.6666 H^+ = 0.8333 Ca^{+2} + 2.1663 H_2O + 1.0000 SiO_2	11.1373	−13.91062	3.064440 × 10^3	5.962965	59
TobJenSS CS100	0.8	0.2	(CaO)1.0000(SiO_2)1.0000(H_2O) 1.4864 + 2.0000 H^+ = 1.0000 Ca^{+2} + 2.4864 H_2O + 1.0000 SiO_2	14.5527	−15.22546	4.186636 × 10^3	6.357638	62.8
TobJenSS CS117	0.6	0.4	(CaO)1.1667(SiO_2)1.0000(H_2O) 1.6398 + 2.3334 H^+ = 1.1667 Ca^{+2} + 2.8065 H_2O + 1.0000 SiO_2	18.1104	−16.39794	5.308832 × 10^3	6.752311	66.6
TobJenSS CS133	0.4	0.6	(CaO)1.3333(SiO_2)1.0000(H_2O) 1.7932 + 2.6666 H^+ = 1.3333 Ca^{+2} + 3.1265 H_2O + 1.0000 SiO_2	21.7431	−17.49397	6.426629 × 10^3	7.146450	70.4
TobJenSS CS150	0.2	0.8	(CaO)1.5000(SiO_2)1.0000(H_2O) 1.9466 + 3.0000 H^+ = 1.5000 Ca^{+2} + 3.4466 H_2O + 1.0000 SiO_2	25.4508	−18.51652	7.548825 × 10^3	7.541123	74.2
Jennite	0	1	(CaO)1.6667(SiO_2)1.0000(H_2O) 2.1000 + 3.3334 H^+ = 1.6667 Ca^{+2} + 3.7667 H_2O + 1.0000 SiO_2	29.3008	−19.39671	8.671021 × 10^3	7.935796	78

Next, appropriate mole fractions were chosen to discretise the solid solutions and create the series of DSPs. In the current paper, mole fraction increments of 0.2 were used to describe the two-end-member CSH model in terms of X_i and X_j, where the sum of the mole fractions in each solid solution had to equal one. Using these mole fractions, the solid phase composition (CaO, SiO_2, H_2O), aqueous reaction components (H^+, Ca^{+2}, H_2O and SiO_2(aq)), mass (g/mol) and volume (cm^3/mol) were determined for each DSP based on the original end-members. The solubility constant was determined for each DSP in the CSH model using Equation (2), where K_i and K_j are the log K values of the end-members.

$$K = (K_i \cdot X_i)^{Xi} \cdot (K_j \cdot X_j)^{Xj} \quad (2)$$

The modelling of OPC hydration required a credible account of the kinetic dissolution of the clinker phases as a function of time [24], the oversaturation of the precipitating hydrate phases during the first 12 h of hydration [25] and the release and uptake of alkali

metals (K and Na) by the C-S-H gel [26]. To minimise the computing time, all input data were defined in an Excel spreadsheet and transferred directly into the PHREEQC input file.

The above shows how the C-S-H gel's solubility could be modelled as a series of DSPs, which, here, were derived from the jennite and tobermorite-II end-members provided in the cemdata07 database. However, a solid solution model was not needed to model the OPC hydration, which, in fact, only required portlandite and a suitable C-S-H gel phase of a fixed calcium to silica (Ca/Si) ratio between 1.6 and 1.8 and a water/Si (H/Si) molar ratio between 2.0 and 2.1. In the DSP model presented in [19], these values were closely matched by the CSH(165) phase, which had a Ca/S ratio of 1.65 and H/Si ratio of 2.1167. As shown in Figure 1, the TobJenSS_CS150 DSP was the only one predicting the precipitation of the C-S-H gel, which, with a Ca/Si ratio of 1.50 and H/Si ratio of 1.947, was not suitable to represent the C-S-H gel in the hydrated OPC. The jennite and tobermorite-II model should, therefore, only be used in cement blends where lower C/S ratios are purposefully targeted by the addition of supplementary cementitious materials (SCMs). Going forward, only the TobJenSS_CS150 phase (Table 2) was used in the analysis to represent the C-S-H gel in the PHREEQC model used here.

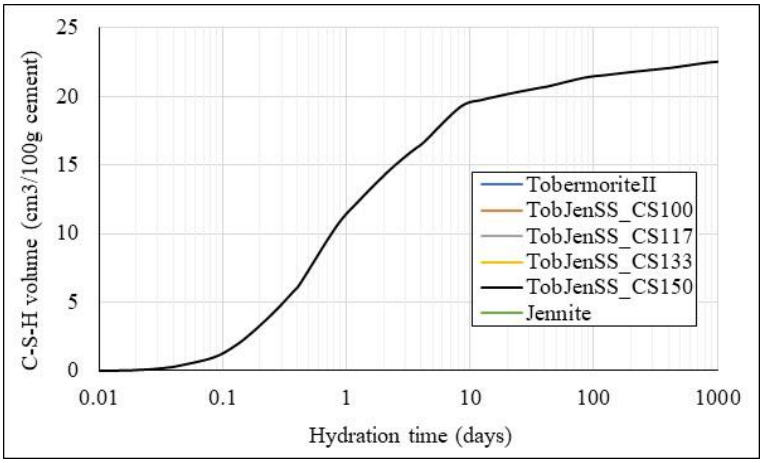

Figure 1. Predicted volume of C-S-H precipitated by each DSP.

Solid solution modelling encompassed all known synthetic ranges of C-S-H gels, which, in fact, were only needed if portlandite was lost and the Ca/Si ratio in the C-S-H gel was lowered, either by the addition of siliceous SCM or by chemical degradation in increasingly larger volumes of leachate provided by the ingress of groundwater or seawater.

3. Thermodynamic Modelling of Cement Hydration

This section described how a full cement hydration simulation could be undertaken using PHREEQC after preprocessing/defining the input in Excel and outputting the results in tabular or graphical formats. The input requirements of the spreadsheet included the definition of the cement composition in terms of oxide proportions of SiO_2, Al_2O_3, Fe_2O_3, CaO, MgO, Na_2O, K_2O, CaO as free lime, CO_2, SO_3 (%), the w/c ratio (−), curing temperature (°C), relative humidity (%) and Blaine fineness (m^2/kg) as per [22] (Table 3).

Table 3. Cement oxide proportions (taken from [20]).

Oxide Proportions (g/100 g Cement)				Phase Compositions (g/100 g Cement)			
OPC		Limestone		OPC		Limestone	
SiO_2	20.2	SiO	0.8	C_3S	66.5	C_3S	64.60
Al_2O_3	4.9	Al_2O_3	0.3	C_2S	10.30	C_2S	9.30
Fe_2O_3	3.2	Fe_2O_3	0.3	C_3A	7.50	C_3A	7.40
CaO	63.9	CaO	55	C_4AF	8.50	C_4AF	7.80
MgO	1.8	MgO	1.8	CaO_free	0.93	CaO-free	0.89
Na_2O	0.42	Na_2O	<0.01	Calcite	0.60	Calcite	4.60
K_2O	0.78	K_2O	<0.01	Gypsum	3.10	Gypsum	3.00
CaO-free	0.93	CaO-free	<0.01	Periclase	0.90	Periclase	0.90
CO_2	0.26	CO_2	42.5	K_2SO_4	1.30	K_2SO_4	1.30
SO_3	2.29	SO_3	0.05	Na_2SO_4	0.21	Na_2SO_4	0.20
Periclase	0.9	Periclase	0.9	Alkali			
Blaine fineness (m^2/kg)				K_2O	0.05	K_2O	0.05
413		429		Na_2O	0.33	Na_2O	0.31
Ignition loss				MgO	0.94	MgO	0.87
0.37		43.4		SO_3	0.11	SO_3	0.11

The spreadsheet defined the required input for every time step up to 1000 days hydration as a series of 47 individual solutions. The time intervals used here allowed for the simulation to be undertaken in a relatively short time. The output from the full analysis could be given in tabular and/or graphical formats. The current output provided included volumes and masses of phase assemblages, clinker dissolution and degree of hydration, Ca/Si ratios in the C-S-H system, pH, pore solution chemistry and ionic strength after each time step. Equilibrium constants at 20 °C were used to describe the dissolution reactions of solid phases and the formation reactions of aqueous species/complexes in the analysis [7,22].

3.1. OPC Clinker Rate Equations

The dissolution of the four main clinker phases was described with the empirical rate equations proposed by [24] and modified by Lothenbach and coworkers [7], using Equations (3)–(5) for any specified time step. In this paper, the empirical expressions and the constants used in their approach can be found in Table 3, described by Lothenbach et al. [22]. A variable time step was used so that, here, only 47 steps were required to predict the dissolution of the four clinker phases for 1000 days of hydration.

$$R_t = \frac{K}{N}(1-\alpha_t)(-ln(1-\alpha_t))^{(1-N)} \cdot \frac{A}{A_0} \cdot exp\left[\frac{E_a^m}{R}\left(\frac{1}{T}-\frac{1}{T_0}\right)\right] \cdot \left(\frac{RH-0.55}{0.45}\right)^4 \cdot f\left(\frac{w}{c}\right) \quad (3)$$

$$R_t = \frac{K(1-\alpha_t)^{\frac{2}{3}}}{1-(1-\alpha_t)^{\frac{1}{3}}} \cdot exp\left[\frac{E_a^m}{R}\left(\frac{1}{T}-\frac{1}{T_0}\right)\right] \cdot \left(\frac{RH-0.55}{0.45}\right)^4 \cdot f\left(\frac{w}{c}\right) \quad (4)$$

$$R_t = K(1-\alpha_t)^N \cdot exp\left[\frac{E_a^m}{R}\left(\frac{1}{T}-\frac{1}{T_0}\right)\right] \cdot \left(\frac{RH-0.55}{0.45}\right)^4 \cdot f\left(\frac{w}{c}\right) \quad (5)$$

$$f\left(\frac{w}{c}\right) = (1+3.333 \cdot (\mathrm{H} \cdot w/c - \alpha_{tot}))^4; \text{ for } \alpha_{tot} > \mathrm{H} \cdot w/c \quad (6)$$

3.2. Dissolution of Oxides Dissolved in OPC Clinker

In addition to determining the clinker proportions, the spreadsheet predefined the molar amounts of the oxide components (K_2O, Na_2O, MgO and SO_3) dissolved in the OPC clinker phases (C_3S, C_2S, C_3A and C_4AF). These were defined using compositions described by [27] in Table 4. The dissolution of the oxide components was then proportional to the dissolution of the OPC clinker phases, as described in the preceding section.

Table 4. Composition and percentages of oxides dissolved in cement clinker phases [20].

Clinker Phase	Oxide							
	K_2O	Na_2O	MgO	SO_3	K_2O (wt.%)	Na_2O (wt.%)	MgO (wt.%)	SO_3 (wt.%)
C_3S	0.1	0.1	1.1	0.1	5.26	7.69	18.33	33.33
C_2S	0.9	0.1	0.5	0.2	47.37	7.69	8.33	67.67
C_3A	0.7	1.0	1.4	0	36.84	76.92	23.33	0
C_4AF	0.2	0.1	3.0	0	10.53	7.69	50.0	0
Total	1.9	1.3	6.0	0.3	100	100	100	100

3.3. Accessory Clinker Phases

The remaining accessory clinker phases, free lime (CaO), calcite ($CaCO_3$), gypsum ($CaSO_4(H_2O)_2$), periclase (MgO), arcanite (K_2SO_4) and thenardite (Na_2SO_4) were allowed to reach equilibrium with the pore solution in the first time step. These minerals were, therefore, immediately available to dissolve and contribute to the formation of hydrate phases. Due to the immediate availability of free lime and periclase, for example, small amounts of portlandite and brucite were precipitated in the first time step. Table 5 shows the modelling approach used for the various clinker phases in the current model, building on the approach used by [28], where the alkalis were not included in the analysis.

Table 5. Modelling approach for the hydration behaviour of the clinker phases.

Clinker Phase	Model Approach
C_3S	Kinetic
C_2S	Kinetic
C_3A	Kinetic
C_4AF	Kinetic
K_2O	Kinetic (dissolved in C_3S, C_2S, C_3A and C_4AF)
Na_2O	Kinetic (dissolved in C_3S, C_2S, C_3A and C_4AF)
MgO	Kinetic (dissolved in C_3S, C_2S, C_3A and C_4AF)
SO_3	Kinetic (dissolved in C_3S and C_2S)
Na_2SO_4	Equilibrium—immediately dissolved during step one
K_2SO_4	Equilibrium—immediately dissolved during step one
Lime	Equilibrium—immediately dissolved during step one
Calcite	Equilibrium—reacting instantaneous equilibrium
Gypsum	Equilibrium—reacting instantaneous equilibrium
Periclase	Equilibrium—immediately dissolved during step one

3.4. Oversaturation

It has been reported in the literature [25] that solutions are oversaturated with respect to gypsum, portlandite, syngenite and ettringite during the first 12 h of cement hydration. To increase the solubility of these phases during the first 12 h of hydration, and to also

include C-S-H and brucite, an oversaturation factor of 0.15(n) was applied, where n is the number of charged species involved in the dissolution reaction (Table 6). Furthermore, as a result, gypsum was inhibited from precipitating, as it would be fully depleted within this 12 h timeframe. In PHREEQC, the oversaturation factor was used as the target saturation index in the EQUILIBRIUM PHASES keyword, which then returned to zero after 12 h of hydration.

Table 6. Number of charged species (n) involved in the dissolution reaction of brucite, TobJenSS_CS150, ettringite, gypsum, portlandite and syngenite phases to account for oversaturation (S.I. = 0.15 · n) during the first 12 h of OPC hydration.

Phase	n	S.I. < 12 h
Brucite	3	0.45
TobJenSS_CS150	4.50	0.68
Ettringite	15	2.25
Gypsum	2	0.30
Portlandite	3	0.45
Syngenite	5	0.75

3.5. Alkalis Binding to the C-S-H

The distribution of the alkali elements K and Na between the pore solution and the C-S-H was defined within the PHREEQC input file using KINETIC and RATES data blocks, which were solved at every time step. The authors of [7,22,25] used a distribution coefficient (kd, mL/g) of 0.42 for both K and Na based on the C-S-H gel having a Ca:Si ratio = 1.8, following the work of [26]. Here, the same distribution ratio used for both alkalis was 0.42 based on [26].

4. Full Hydration Analysis Using Cemdata07

Using a w/c ratio of 0.4, a temperature of 20 °C and the cement described in [20] and Table 3, the predicted phase assemblages from the PHREEQC model using the input above are shown in Figure 2. As can be seen in Figure 3, there was an excellent similarity between it and the phase assemblages from [20] in terms of the clinker and gypsum dissolution and solid hydrate phase formation, which was supported by experimental data in [20]. As can be seen, the AFm phase was predominately monosulphate in the OPC and monocarbonate in the LS, which, along with the amount of sulphates (SO_4) available for the reaction, affected the stability of ettringite over time. Previous work [29–31] has shown that the formation of monosulphate, ettringite, hemicarbonate, monocarbonate and/or calcite is controlled by the available molar ratios of SO_3/Al_2O_3 and CO_2/Al_2O_3. The differences in the AFt and AFm phase precipitation could be better seen in Figure 4. As discussed, the presence of calcite promoted the formation of monocarbonate and stabilised ettringite, where the precipitation of monosulphate in the OPC caused it to destabilise. A detailed review of the change in solid hydrates within the two cements can be found in [20].

Figures 4 and 5 present the pore solution chemistry including pH over time, respectively, expected for the two cements using PHREEQC and compared with the experimentally determined values in [20]. As expected, there was reasonably good comparisons between the model and the measured values and trends, with minor differences overall. The pH predictions only varied by ±0.15 pH units, which was well within the uncertainty range of very high pH measurements.

Thermodynamics resulted in cement hydration modelling becoming credible due to the pioneering work by Glasser [32–38] and Lothenbach and coworkers [7,22,25], and this work added another tool to further our understanding of the complex chemical reactions in cementitious systems. Previous work by the authors showed how volume stoichiometries can provide predictions, but failed to include the complex chemical interactions that exist when cement is hydrating, which thermodynamics can reasonably easily incorporate.

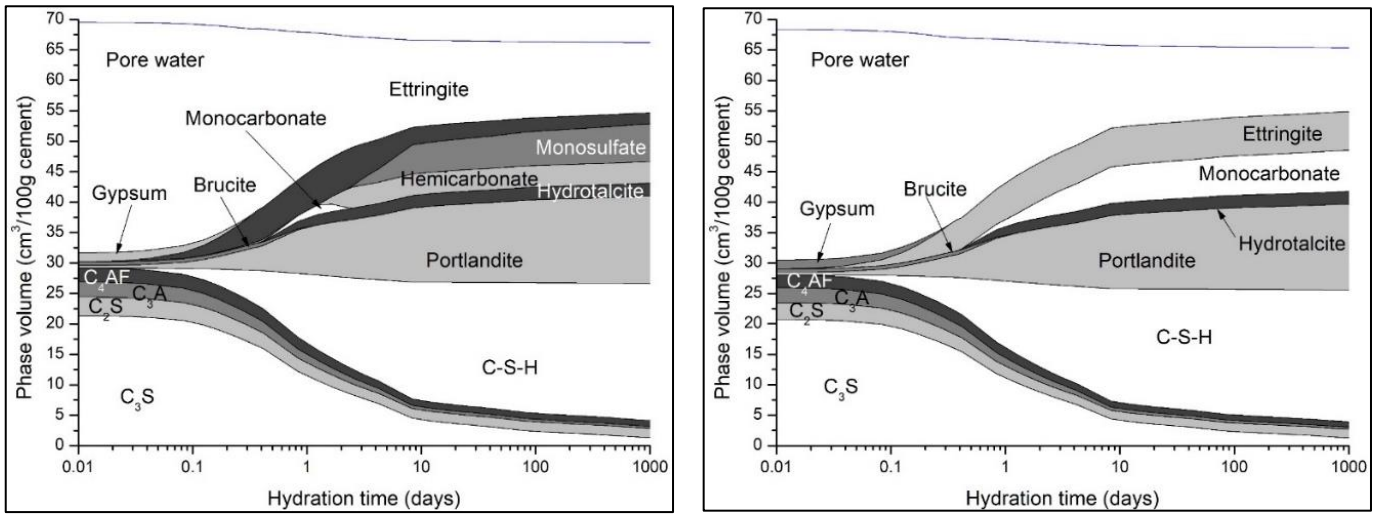

Figure 2. Phase assemblage produced by the PHREEQC model using [20] for the two cements. (**a**) OPC phase assemblage; (**b**) 4% limestone binder phase assemblage.

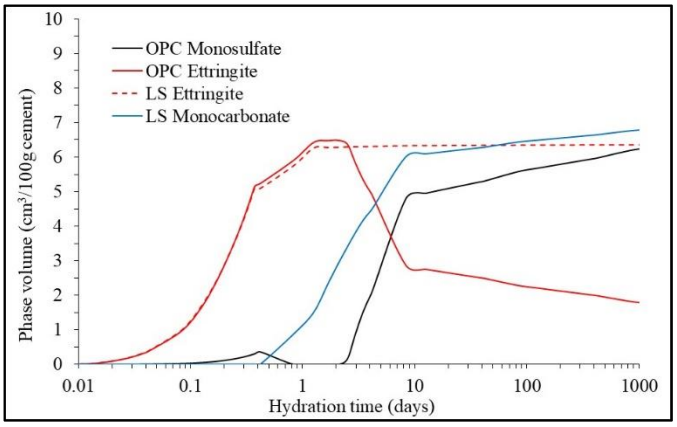

Figure 3. Predicted precipitation of AFt and AFm phases in the two cements described in Table 3.

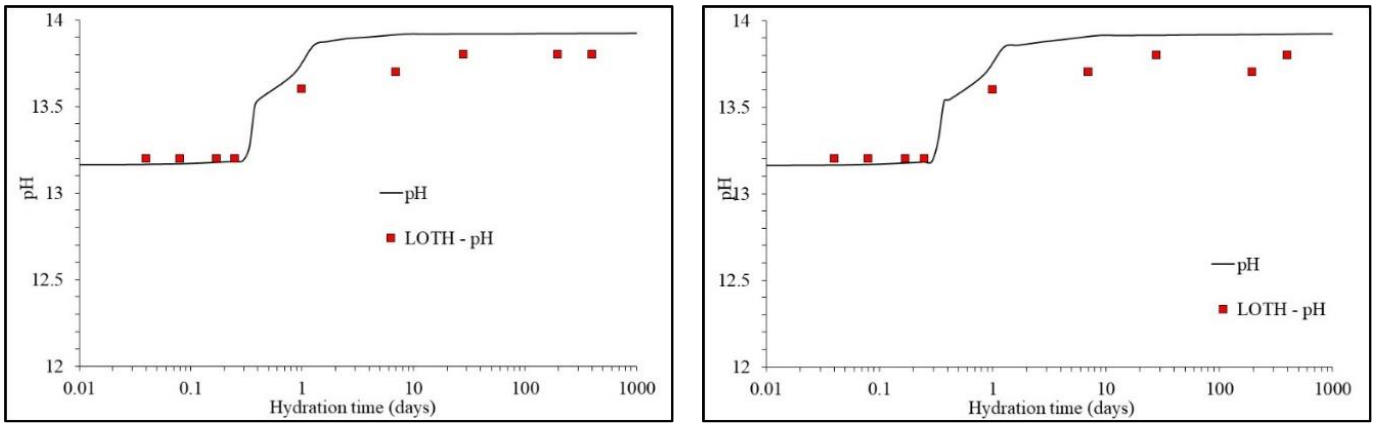

Figure 4. pH predictions for (**a**) OPC and (**b**) 4% limestone binder (LOTH represents the measured data from [20]). (**a**) OPC pH; (**b**) 4% limestone pH.

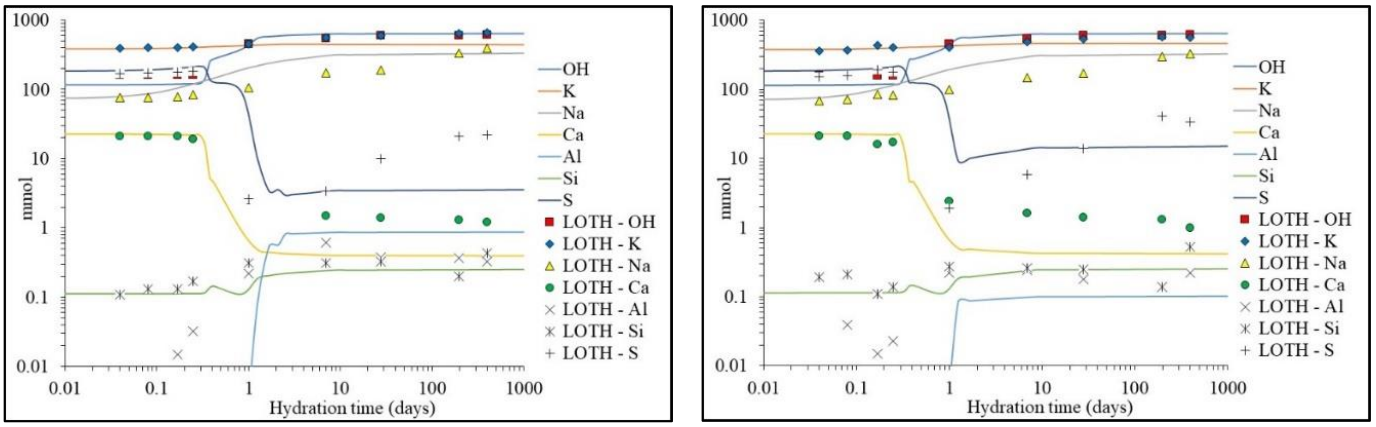

(**a**) (**b**)

Figure 5. Pore solution chemistry produced by the PHREEQC model using [20] for (**a**) OPC and (**b**) 4% limestone binder (LOTH represents the measured data from [20]). (**a**) OPC pore chemistry; (**b**) 4% limestone pore chemistry.

5. Conclusions

This work described the derivation of a series of DSPs to describe the incongruent dissolution of C-S-H gel from the jennite and tobermorite-II end-members provided in the cemdata07 database. While solid solution modelling is possible in PHREEQC, it carries an inherent time and computational load. By using the DSP C-S-H gel solubility models, the computational demand and time were significantly lower and were often completed in less than a minute with no loss in accuracy. In the current work, it was demonstrated that only one of the DSPs derived to model the C-S-H gel phase was required as the Ca/Si and H/Si ratios were suitable for the cement blends herein. While the use of solid solutions and the derivation of DSPs was a thermodynamically credible approach to simulate the incongruent solubility behaviour of C-S-H gel, they were only needed for hydrating cements incorporating SCMs or those undergoing chemical attack.

It was shown that PHREEQC could be used to accurately model cement hydration for Portland cement systems with various amounts of limestone. In these simulations, we predicted the governing dissolution/precipitation reactions accounting for oxide components dissolved in the clinker phases and the represented time-dependent oversaturation and alkali binding to C-S-H by defining the input for PHREEQC in a spreadsheet and pasting it into the input file, which was more efficient, giving the user full control.

Author Contributions: Conceptualization, N.H. and M.T.; methodology, N.H.; software, D.K. and N.H.; validation, M.T.; formal analysis, N.H. and D.K.; investigation, N.H.; data curation, N.H.; writing—original draft preparation, N.H.; writing—review and editing, M.T. and D.K. All authors have read and agreed to the published version of the manuscript.

Funding: Funding to publish this work was from a US–Ireland grant trifunded by the National Science Foundation (NSF, 1805818), Science Foundation Ireland (SFI, 17/US/3424) and the Department for the Economy of Northern Ireland (DfE, USI 127).

Institutional Review Board Statement: Not applicable.

Informed Consent Statement: Not applicable.

Data Availability Statement: Not applicable.

Acknowledgments: The authors would like to acknowledge the advice provided by Colin Walker during the production of this paper.

Conflicts of Interest: The authors declare no conflict of interest.

References

1. Holmes, N.; Tyrer, M.; West, R.P.; Lowe, A.; Kelliher, D. Using PHREEQC to model cement hydration. *Constr. Build. Mater.* **2022**, *319*, 126–129. [CrossRef]
2. Parkhurst, D.J.; Appelo, C.A.J. *Description of Input and Examples for PHREEQC Version 3—A Computer Program for Speciation, Batch-Reaction, One-Dimensional Transport and Inverse Geochemical Calculations*; The U.S. Department of the Interior and the U.S. Geological Survey: Baltimore, MD, USA, 2013.
3. Elakneswaran, Y.; Ishida, T. Development and Verification of an Integrated Physicochemical and Geochemical Modelling Framework for Performance Assessment of Cement-Based Materials. *J. Adv. Concr. Technol.* **2014**, *12*, 111–126. [CrossRef]
4. Maekawa, K.; Ishida, T.; Kishi, T. *Multiscale Modeling of Structural Concrete*; Taylor & Francis: Abingdon, UK, 2009.
5. Elakneswaran, Y.; Owaki, E.; Miyahara, S.; Ogino, M.; Maruya, T.; Nawa, T. Hydration study of slag-blended cement based on thermodynamic considerations. *Constr. Build. Mater.* **2016**, *124*, 615–625. [CrossRef]
6. Charlton, S.R.; Parkhurst, D.L. Modules based on the geochemical model PHREEQC for use in scripting and programming languages. *Comput. Geosci.* **2011**, *37*, 1653–1663. [CrossRef]
7. Lothenbach, B.; Matschei, T.; Glasser, G.; Möschner, F. Thermodynamic modelling of the effect of temperature on the hydration and porosity of Portland cement. *Cem. Concr. Res.* **2008**, *38*, 1–18. [CrossRef]
8. Elakneswaran, Y.; Owaki, E.; Nawa, T. Modelling Long-Term Durability Performance of Cementitious Materials under Sodium Sulphate Interaction. *Appl. Sci.* **2018**, *8*, 2597. [CrossRef]
9. Elakneswaran, Y.; Li, C.; Kajio, T.; Owaki, E.; Ogino, M.; Nawa, T. Durability of slag-blended cement due to U-phase instability in sulphate environment. *Mater. Struct.* **2020**, *53*, 146. [CrossRef]
10. Krishnya, S.; Yoda, Y.; Elakneswaran, Y. A two-stage model for the prediction of mechanical properties of cement paste. *Cem. Concr. Compos.* **2021**, *115*, 103853. [CrossRef]
11. Walker, C.; Savage, D.; Tyrer, M.; Ragnarsdottir, K. Non-ideal solid solution aqueous solution modeling of synthetic calcium silicate hydrate. *Cem. Concr. Res.* **2007**, *37*, 502–511. [CrossRef]
12. Curti, E. Coprecipitation of radionuclides with calcite: Estimation of partition coefficients based on a review of laboratory investigations and geochemical data. *Appl. Geochem.* **1999**, *14*, 433–445. [CrossRef]
13. Atkinson, A.; Hearne, J.A.; Knights, C.F. Aqueous chemistry and thermodynamic modelling of CaO-SiO_2-H_2O gels. *J. Chem. Soc. Dalton Trans.* **1989**, 2371–2379.
14. Aimoz, L.; Kulik, D.A.; Wieland, E.; Curti, E.; Lothenbach, B.; Mader, U. Thermodynamics of AFm-(I_2,SO_4) solid solution and of its end-members in aqueous media. *Appl. Geochem.* **2012**, *27*, 2117–2129. [CrossRef]
15. Dilnesa, B.Z.; Lothenbach, B.; le Saout, G.; Renaudin, G.; Mesbah, A.; Filinchuk, Y.; Wichser, A.; Wieland, E. Iron in carbonate containing AFm phases. *Cem. Concr. Res.* **2011**, *41*, 311–323. [CrossRef]
16. Hobbs, M.Y. Solubilities and ion exchange properties of solid solutions between the OH, Cl and CO_3 end members of the monocalcium aluminate hydrates. Ph.D. Thesis, University of Waterloo, Waterloo, ON, Canada, 2001; p. 226.
17. Möschner, G.; Lothenbach, B.; Winnefeld, F.; Ulrich, A.; Figi, R.; Kretzschmar, R. Solid solution between Al-ettringite and Fe-ettringite ($Ca_6[Al_1-xFex(OH)6]2(SO_4)3{\cdot}26H_2O$). *Cem. Concr. Res.* **2009**, *39*, 482–489. [CrossRef]
18. Dilnesa, B.Z.; Lothenbach, B.; Renaudin, G.; Wichser, A.; Kulik, D.A. Synthesis and characterization of hydrogarnet Ca_3(AlxFe$_1$-x)2(SiO_4)y(OH)4(3-y). *Cem. Concr. Res.* **2014**, *59*, 96–111. [CrossRef]
19. Walker, C.; Sutou, S.; Oda, C.; Mihara, M.; Honda, A. Calcium silicate hydrate (C-S-H) gel solubility data and a discrete solid phase model at 25 °C based on two binary non-ideal solid solutions. *Cem. Concr. Res.* **2016**, *79*, 1–30. [CrossRef]
20. Svenum, I.-H.; Ringdalen, I.G.; Bleken, F.L.; Friis, J.; Höche, D.; Swang, O. Structure, hydration, and chloride ingress in C-S-H: Insight from DFT calculations. *Cem. Concr. Res.* **2020**, *129*, 105965. [CrossRef]
21. BWong, M.; Lacina, D.; Nielsen, I.M.B.; Graetz, J.; Allendorf, M.D. Thermochemistry of Alane Complexes for Hydrogen Storage: A Theoretical and Experimental Investigation. *J. Phys. Chem. C* **2011**, *115*, 7778–7786. [CrossRef]
22. Lothenbach, B.; le Saout, G.; Gallucci, E.; Scrivener, K. Influence of limestone on the hydration of Portland cements. *Cem. Concr. Res.* **2008**, *38*, 848–860. [CrossRef]
23. Lothenbach, B.; Kulik, D.A.; Matschei, T.; Balonis, M.; Baquerizo, L.; Dilnes, B.; Miron, G.D.; Myers, R.J. Cemdata18: A chemical thermodynamic database for hydrated Portland cements and alkali-activated materials. *Cem. Concr. Res.* **2019**, *115*, 472–506. [CrossRef]
24. Killoh, L.J.; Parrot, D.C. Prediction of cement hydration. *Br. Ceram. Proc.* **1984**, *35*, 41–53.
25. Winnefeld, F.; Lothenbach, B. Thermodynamic modelling of the hydration of Portland Cement. *Cem. Concr. Res.* **2006**, *36*, 209–226.
26. Hong, S.Y.; Glasser, F.P. Alkali binding in cement pastes: Part I. The C-S-H phase. *Cem. Concr. Res.* **1999**, *29*, 1893–1903. [CrossRef]
27. Taylor, H.F.W. *Cement Chemistry*; Thomas Telford Publishing: London, UK, 1997.
28. Savage, D.; Soler, J.M.; Yamaguchi, K.; Walker, C.; Honda, A.; Inagaki, M.; Watson, C.; Wilson, J.; Benbow, S.; Gaus, I.; et al. A comparative study of the modelling of cement hydration and cement–rock laboratory experiments. *Appl. Geochem.* **2011**, *26*, 1138–1152. [CrossRef]
29. de Weerdt, K.; Haha, M.B.; le Saout, G.; Kjellsen, K.O.; Justnes, H.; Lothenbach, B. Hydration mechanisms of ternary Portland cements containing limestone powder and fly ash. *Cem. Concr. Res.* **2011**, *41*, 279–291. [CrossRef]
30. Lothenbach, B.; Damidot, D.; Marchand, T.; Matschei, T. Thermodynamic modelling: State of knowledge and challenges. *Adv. Cem. Res.* **2010**, *22*, 211–223. [CrossRef]
31. Matschei, T.; Lothenbach, B.; Glasser, F.P. The role of calcium carbonate in cement hydration. *Cem. Concr. Res.* **2007**, *37*, 551–558. [CrossRef]

32. Atkins, M.; Bennett, D.G.; Dawes, A.C.; Glasser, F.P.; Kindness, A.; Read, D. A thermodynamic model for blended cements. *Cem. Concr. Res.* **1992**, *22*, 497–502. [CrossRef]
33. Bennett, D.G.; Read, D.; Atkins, M.; Glasser, F.P. A thermodynamic model for blended cements. II: Cement hydrate phases; thermodynamic values and modelling studies. *J. Nucl. Mater.* **1992**, *190*, 315–325. [CrossRef]
34. Damidot, D.; Glasser, F.P. Thermodynamic investigation of the CaO Al_2O_3 $CaSO_4$ H_2O system at 50°C and 85 °C. *Cem. Concr. Res.* **1992**, *22*, 1179–1191. [CrossRef]
35. Damidot, D.; Glasser, F.P. Thermodynamic investigation of the CaO Al_2O_3 $CaSO_4$ K_2O H_2O system at 25 °C. *Cem. Concr. Res.* **1993**, *23*, 1195–1204. [CrossRef]
36. Damidot, D.; Glasser, F.P. Thermodynamic investigation of the CaO Al_2O_3 $CaSO_4$ H_2O system at 25 °C and the influence of Na_2O. *Cem. Concr. Res.* **1993**, *23*, 221–238. [CrossRef]
37. Damidot, D.; Stronach, S.; Kindness, A.; Atkins, M.; Glasser, F.P. Thermodynamic investigation of the CaO_Al_2O_3_$CaCO_3$-H_2O closed system at 25 °C and the influence of Na_2O. *Cem. Concr. Res.* **1994**, *24*, 563–572. [CrossRef]
38. Atkins, M.; Glasser, F.P.; Kindness, A. Cement hydrate phases: Solubility at 25 °C. *Cem. Concr. Res.* **1992**, *22*, 241–246. [CrossRef]